



HAL
open science

Efficient ultraviolet light frequency down-shifting by a thin film of ZnO nanoparticles

Aleksandra Apostoluk, Bruno Masenelli, Elsa Tupin, Bruno Canut, Dimitri Hapiuk, Patrice Melinon, Jean-Jacques Delaunay

► To cite this version:

Aleksandra Apostoluk, Bruno Masenelli, Elsa Tupin, Bruno Canut, Dimitri Hapiuk, et al.. Efficient ultraviolet light frequency down-shifting by a thin film of ZnO nanoparticles. International Journal of Nanoscience, 2012, Selected Invited Papers from the Bilateral Conference between Canadian and French Researchers in Nanofabrication and Nanoscience;, 11 (04), pp.1240022. 10.1142/S0219581X12400224 . hal-01965022

HAL Id: hal-01965022

<https://hal.science/hal-01965022>

Submitted on 17 Jan 2022

HAL is a multi-disciplinary open access archive for the deposit and dissemination of scientific research documents, whether they are published or not. The documents may come from teaching and research institutions in France or abroad, or from public or private research centers.

L'archive ouverte pluridisciplinaire **HAL**, est destinée au dépôt et à la diffusion de documents scientifiques de niveau recherche, publiés ou non, émanant des établissements d'enseignement et de recherche français ou étrangers, des laboratoires publics ou privés.



Distributed under a Creative Commons Attribution - NonCommercial 4.0 International License

EFFICIENT ULTRAVIOLET LIGHT FREQUENCY DOWN-SHIFTING BY A THIN FILM OF ZnO NANOPARTICLES

ALEKSANDRA APOSTOLUK*, BRUNO MASENELLI,
ELSA TUPIN and BRUNO CANUT
*Institut des Nanotechnologies de Lyon
INL, CNRS–UMR 5270, INSA–Lyon
Villeurbanne, F–69621, France
aleksandra.apostoluk@insa–lyon.fr

DIMITRI HAPIUK and PATRICE MÉLINON
*Laboratoire de Physique de la Matière
Condensée et Nanostructures, LPMCN, CNR–UMR 5586
Université Claude Bernard Lyon 1
Villeurbanne, F–69622, France*

JEAN-JACQUES DELAUNAY
*School of Engineering, The University of Tokyo
7-3-1 Hongo, Bunkyo-ku, Tokyo 113-8656, Japan*

The maximal efficiency of a single junction solar cell (SC) is defined as the Shockley–Queisser limit, which determines the maximal output power which can be furnished by a SC as a function of the bandgap of the semiconductor constituting the cell. The short wavelength spectral response of a SC can be improved if a luminescent down-converting layer is added to the SC structure. We propose the use of a layer containing ZnO nanoparticles (NPs) as a luminescent down-shifter. ZnO is able to absorb efficiently the ultraviolet light ($\lambda < 400$ nm), where the SC spectral response is low and to re-emit lower energy photons (longer wavelength photons) for which the SC spectral response is enhanced, thus increasing the total photocurrent. The stoichiometry and crystallinity of ZnO NPs can be controlled and adjusted to obtain the highest visible photoluminescent emission, indicator of an efficient down-shifting. The ratio between the ZnO UV absorption and visible emission is also estimated and from these results we expect the increase of the SC efficiency using ZnO NPs as a down-shifting layer placed on the front side of the SC.

Keywords: Zinc oxide; nanoparticles; photoluminescence; down-shifting; solar cell.

1. Introduction

Theoretical maximal efficiency of a single junction solar cell (SC) is referred as the Shockley–Queisser limit¹ and mainly depends on the matching between the solar emission spectrum and the absorption spectrum of the semiconducting material constituting the SC active layer. It places the maximum solar conversion efficiency at around 31% for a $p-n$ junction made of a material having a bandgap of 1.1–1.3 eV (Si or other widely used semiconductors). In a standard silicon single-junction solar cell only a part of the solar emission spectrum is absorbed: the semiconductor is transparent to the lower energy photons and another fraction of the sun light is lost due to the thermalization phenomenon of highly energetic (short wavelength) photons.

The maximal SC efficiency is limited by its optical absorption, surface reflection, carrier transport and carrier collection. A wide range of approaches was proposed to surpass this efficiency limit: the development of tandem SCs, optical excitation through midgap defect levels, interband transitions, fluorescent down-conversion (DC)² or down-shifting (DS), or thermophotovoltaic DC.³

Because of its optical and electrical properties, ZnO is a very attractive wide bandgap semiconductor and has multiple applications in photo-electrical and optoelectronic devices. Unlike other wide bandgap materials, it is relatively inexpensive, abundant, chemically stable, easy to fabricate, non-toxic and benefits from rather simple crystal growth technology. This results in lower fabrication costs of ZnO-based devices. It has a bandgap of 3.37 eV ($\lambda \approx 367$ nm) at room temperature (RT), close to that of GaN (about 3.4 eV at RT). Moreover, ZnO has a larger exciton binding energy than GaN (60 meV, 2.4 times larger than kT at RT), which results in bright UV luminescence emission from free excitons at RT. In the case of the ZnO nanoparticles (NPs) with perfect crystallinity, only this ultraviolet excitonic luminescence is observed, when excited with a UV laser above the ZnO bandgap. Our idea is to enhance the green and red luminescence of the ZnO NPs to the detriment of their UV excitonic emission and apply them as a down-shifting layer placed on the front side of a SC. This green–red PL emission enhancement can be achieved by deliberate introduction of oxygen defects in ZnO NP crystal structure, thus making them to be non-stoichiometric.

ZnO application in SCs is not a new concept: ZnO:Al doped (AZO) layers have been used as a transparent electrode in the silicon SCs,⁴ as an antireflective index-matching coating⁵ and ZnO nanorods and NPs were used an active layer in hybrid SCs.^{6,7}

Another material proposed as a down-converter in SCs is CdS,⁸ but the use of cadmium compounds is still problematic due to their high toxicity.

We propose the application of a film of ZnO NPs as a down-shifting layer to be placed on the front side of a pre-existing commercial SC. This down-shifting layer permits to generate one low-energy photon for every incident high-energy photon, thus limiting the front surface recombination of hot photocarriers and thereby enhance the photocurrent generation and the overall conversion efficiency of a SC.

2. Experimental Details

2.1. *Fabrication of ZnO nanoparticles*

ZnO NPs were fabricated using an original and purely physical method performed in the gas phase: the low energy cluster beam deposition (LECBD).⁹ The nanoparticle’s final size (between 6 and 18 nm) is influenced by the nozzle shape, chamber volume, and the laser fluence. The NPs’ stoichiometry, crystallinity and surface quality can be adjusted via the control of the LECBD synthesis parameters.

A cluster generator based on a combined Nd:YAG laser vaporization and a rare gas (Ar) condensation source is used to deliver a supersonic jet of NPs with sizes ranging from a few tens to some thousands of atoms (diameters varying from 2 nm to a few nm). The target is a stoichiometric ZnO powder (99.99% pure) which was pressed and heated in a furnace at 1173 K under oxygen atmosphere for 8 h. The oxygen is injected in the Ar flux present in the nucleation chamber. Different values of the oxygen partial pressure as compared to the Ar pressure were applied in order to obtain the ZnO NPs with diverse stoichiometry. It should be noted that the deposited ZnO cluster assembly has the same stoichiometry as the plasma. The nucleation process occurs in a supersonic nozzle, where the atoms are hyper-quenched beyond the thermodynamic equilibrium. The study by transmission electron microscopy (TEM) and X-ray diffraction shows that the NPs are crystallized in the wurtzite structure. Figure 1 presents a high resolution TEM

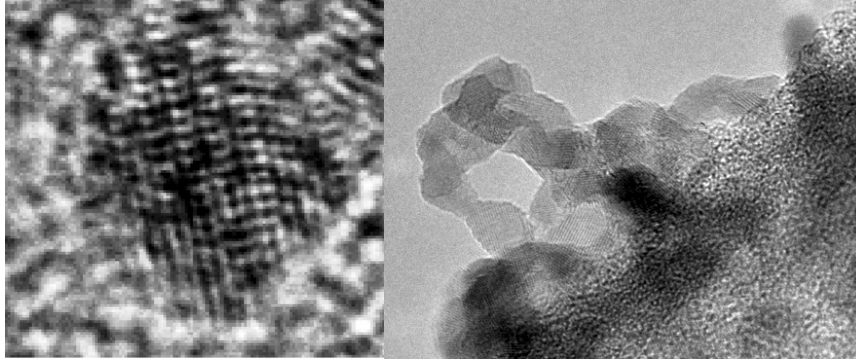


Fig. 1. On the left, a high-resolution TEM image of one ZnO nanoparticle (the image size is $6.3\text{ nm} \times 6.3\text{ nm}$), the crystalline structure can be clearly seen; the average size of one NP is 6 nm . On the right, an assembly of several NPs, illustrating the foam-like structure of the deposited ZnO NP film.

image of a ZnO individual NP. The obtained ZnO NP films are very porous ($\sim 70\%$), so we can say that a sort of a foam is fabricated via the LECBD process (cf. Fig. 1 on the right).

2.2. Absorption and reflectivity measurement

The absorption and reflectivity of the ZnO NP layers were measured using a double beam Perkin Elmer Lambda 900 UV/VIS/NIR spectrometer using pre-aligned tungsten–halogen and deuterium lamps as sources.

2.3. Rutherford backscattering spectrometry study

The atomic composition and areal mass of the ZnO NPs films were studied by Rutherford backscattering spectrometry (RBS). The measurements were performed using a beam of $^4\text{He}^+$ ions of 2 MeV energy delivered by the 4 MV Van de Graaff accelerator of the Nuclear Physics Institute of Lyon (IPNL). The backscattered particles were detected with a 13 keV -resolution implanted Si junction, set at an angle of 172° with respect to the incident ion beam axis.

2.4. Photoluminescence study

The RT photoluminescence (PL) experiments were performed with a frequency doubled argon laser operating at 244 nm (Lexel 95 SHG). The PL signal of ZnO NPs was dispersed using a Jobin–Yvon HR 640 monochromator with a 600 lines/mm grating blazed at 400 nm and then detected with a GaAs

(Hamamatsu H5701–50) photomultiplier. In all cases the spectra are corrected from the spectral response of the system and normalized to their maximum.

3. Experimental Results

It has been already demonstrated that depending on the method of the incorporation of oxygen into the NPs during the LECBD process, clusters with identical stoichiometry exhibit very different PL properties.⁹ The post-deposition exposition to oxygen does not improve in a significant manner the stoichiometry of the ZnO NPs.¹⁰ Thus, for the fabrication of non-stoichiometric ZnO NPs having efficient green and red luminescence (necessary for DC), we need to vary the oxygen pressure in the plasma *during* the LECBD process.

We observed that the ratio between the excitonic and the green–red PL emission band can be adjusted via the variation of the value of the partial oxygen pressure in the plasma applied during the LECBD of the ZnO NPs.¹¹ ZnO NPs deposited as thin porous layers (several tenths of nm thick) under various oxygen partial pressures were studied: 25% of the oxygen in the buffer gas (resulting in stoichiometric ZnO_x NPs, $x = 1$), then 12.5% and 7% of the oxygen in the buffer gas (these last two values resulted in nonstoichiometric ZnO_x , with theoretical values of $x = 0.5$ and 0.28 , respectively, as deduced from the calibration based on the X-ray photoelectron spectroscopy (XPS) measurements¹⁰).

The stoichiometry and areal mass of the fabricated NPs were measured by RBS. It showed that in the case of all studied samples nanoparticles *are* stoichiometric ($x = 1$), though the LECBD

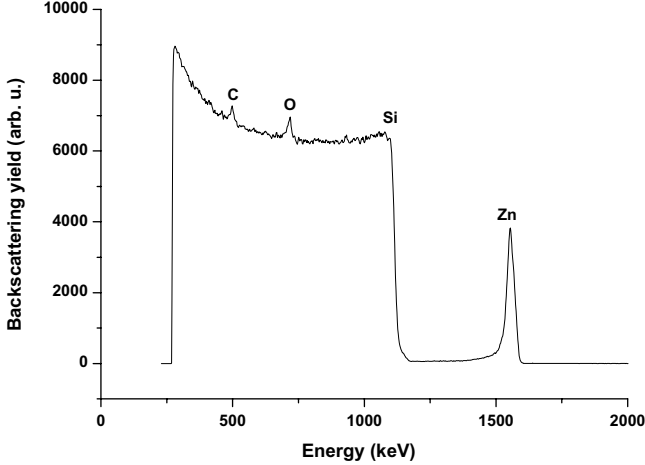


Fig. 2. RBS spectrum recorded on ZnO_x NPs with a theoretical value of $x = 0.28$. The RBS measurements indicate that within the experimental uncertainties, the deposited NPs are stoichiometric (measured value: $x = 1$) and their areal mass is $7.8 \mu\text{g} \cdot \text{cm}^{-2}$. Analysis conditions: $^4\text{He}^+$ ions of 2 MeV energy; detection angle of 172° .

parameters used during the fabrication of the two of them (these deposited with 12.5% and 7% of the oxygen in the buffer gas) should permit to fabricate the ZnO NPs with oxygen vacancies (thus non-stoichiometric ZnO_x). In the RBS spectrum shown in Fig. 2, the expected oxygen content was $x = 0.28$. The only “unusual” peak observed in this spectrum is the carbon signal. It indicates that there was some residual pollution present on the studied sample. The LECBD plasma parameters (oxygen and argon partial pressures), the theoretical oxygen content and oxygen content measured by RBS for all studied samples are summarized in Table 1.

All ZnO NPs films were exposed to the ambient air after deposition and as they are very porous, we concluded that the oxygen adsorption at the NPs surface occurred. This adsorbed oxygen filled the oxygen vacancies at the NPs surface. High roughness and porosity of the ZnO NPs films (which facilitates oxygen adsorption) are evidenced in the low energy tail of the Zn peak observed in the RBS spectrum presented in Fig. 2. It should be also noted that the intensity of the defect-related emission of the PL spectrum (between ~ 1.7 eV and ~ 3.1 eV) of the ZnO NPs was increased after the exposition of the NPs to the ambient air.¹¹

The influence of the oxygen partial pressure applied during the LECBD on the enhancement of the green and red luminescence emitted by ZnO NPs was studied by the UV-excited PL at RT. The

Table 1. Parameters of the plasma used during the ZnO NPs deposition by the LECBD technique, resulting theoretical ZnO_x stoichiometries (as deduced from the calibration based on the XPS measurements¹⁰) and the content of each element (Zn and O) detected by RBS (the RBS measurement error is $\pm 2\%$).

Oxygen partial pressure in the LECBD plasma	1.4 mbar	2.5 mbar	5 mbar
Argon partial pressure in the LECBD plasma	18.6 mbar	17.5 mbar	15 mbar
Theoretical oxygen content x in ZnO_x	$x = 0.28$	$x = 0.5$	$x = 1$
ZnO nanoparticles theoretically stoichiometric?	No	No	Yes
Oxygen content (x) measured by RBS	1.04	1	1.02

absorption and reflectance of the ZnO NP layers were also measured in order to determine the ability of ZnO NPs of the efficient light harvesting and down-shifting. The ZnO NP film absorption is presented in Fig. 3, together with the UV-visible conversion quantum yield.

In order to estimate the conversion quantum yield of the ZnO NPs, at first we studied the PL excited with a UV laser at 244 nm in function of the LECBD parameters. Two PL peaks were observed for all samples — the excitonic emission in the UV (at 378 nm) and the defect-related green–red lumi-

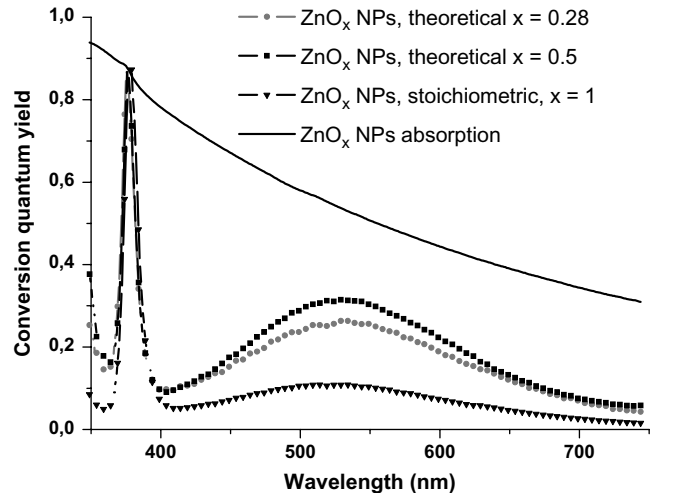


Fig. 3. The conversion quantum yield of the ZnO_x NPs as a function of their theoretical stoichiometry (calculated from the LECBD plasma composition and using the calibration based on the XPS measurement¹⁰). It can be clearly noticed that the maximum UV–visible conversion efficiency is observed for the sample with a theoretical stoichiometry of $x = 0.5$. The absorption spectrum of the ZnO NP layer is also shown.

nescence.¹¹ This visible PL is due to the oxygen vacancies in the ZnO crystal lattice. We clearly observed the enhancement of the green and red emission in non-stoichiometric ZnO NPs, when compared to the PL signal from the stoichiometric ones.¹¹ The excitonic contribution to the PL signal, located at 378 nm (~ 3.28 eV) was already observed for other ZnO nanostructures. The defect-related green luminescence band is generally observed around 530 nm. It should also be noted that the ratio between the excitonic and the defect related emission is often used as an indirect probe of the ZnO film crystalline quality.

The stronger green–red emission, the better will be down-shifting in ZnO, as it is a proof that it absorbs the UV light and emits the green–red light efficiently. The highest green–red PL intensity was observed in the case of the ZnO_x NP film for which the theoretical value of $x = 0.5$ (which corresponds to 12.5% oxygen in the plasma in the LECBD¹¹). Thus we concluded that there exists an optimal partial oxygen pressure in the buffer gas (plasma) injected during the LECBD, which permits to obtain the ZnO NPs of poor crystalline quality, with many oxygen vacancies present in the crystal structure.

We quantified the UV-visible conversion quantum yield in the ZnO NP film (shown in Fig. 3 together with the ZnO NP film absorption) assuming that all absorbed UV photons are re-emitted in a radiative manner (i.e. there is not any non-radiative recombination), which is of course an ideal situation. Obtained results suggests that for some reason the ZnO_x with the theoretical value of $x = 0.5$ (as deduced from the calibration based on the XPS¹⁰) is better for the DC than the ZnO_x with $x = 0.28$. As can be noticed in Fig. 3, the maximal value of the UV-visible conversion efficiency in the ideal case, where the radiative recombination is the only possible way of disexcitation, is estimated at about 30%, though this value should be confirmed by the measurements of the efficiencies of the final photovoltaic devices.

4. Conclusions and Perspectives

In this paper, ZnO NPs deposited by a purely physical method — the LECBD — were studied. The crystalline quality of the fabricated NPs was proven by the HRTEM analysis. The NP size is of

about 6 nm. Two contributions to the PL emission spectrum of ZnO NPs were observed — the excitonic one at around 378 nm and the defect-related one in the 400–700 nm spectral range. We quantified the ZnO NP film conversion quantum yield and it turned out to be of about 30% in the UV-visible region. Further work will concern the application of these ZnO NPs as a down-shifting layer placed on the front side of a commercially available silicon solar cell, and we expect the increase of the efficiency of such a device.

Acknowledgments

The ZnO nanoparticles we studied were fabricated using the research facilities of the PLYRA (Plateforme LYonnaise de Recherche sur les Agrégats) platform at the Lyon 1 university. The authors acknowledge Olivier Boisron for his kind assistance during the ZnO nanoparticle layer deposition.

References

1. W. Shockley and H. J. Queisser, *J. Appl. Phys.* **32**, 510 (1961).
2. A. S. Brown and M. A. Green, *J. Appl. Phys.* **92**, 1329 (2002).
3. B. Jalali, S. Fathpour and K. Tsia, *Opt. Photonics News* **20**, 18 (2009).
4. Z. C. Zin, I. Hamberg and C. G. Granqvist, *J. Appl. Phys.* **64**, 5117 (1988).
5. Y.-J. Lee, D. S. Ruby, D. W. Peters, B. B. McKenzie and J. W. P. Hsu, *Nano Lett.* **8**, 1501 (2008).
6. W. J. E. Beek, M. M. Wienk and R. A. J. Janssen, *Adv. Mater.* **16**, 1009 (2004).
7. W. J. E. Beek, M. M. Wienk, M. Kemerink, X. Yang and R. A. J. Janssen. *J. Phys. Chem. B* **109**, 9505 (2005).
8. M. S. Saidov, *Appl. Sol. Energy* **43**, 161 (2007).
9. A. Perez, P. Mélinon, V. Dupuis, P. Jensen, B. Prevel, J. Tuillon, L. Bardotti, C. Martet, M. Treilleux, M. Broyer, M. Pellarin, J. L. Vaille, B. Palpant and J. Lerme, *J. Phys. D: Appl. Phys.* **30**, 709 (1997).
10. D. Tainoff, B. Masenelli, O. Boisron, G. Guiraud and P. Mélinon, *J. Phys. Chem. C* **112**, 12623 (2008).
11. A. Apostoluk, B. Masenelli, Y. Zhu, B. Canut, D. Hapiuk and J. J. Delaunay, paper in preparation.